

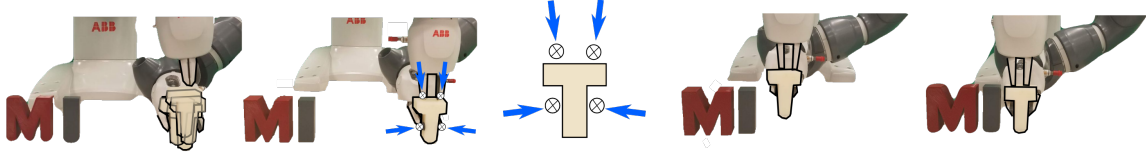
# A Convex-Combinatorial Model for Planar Caging

Bernardo Aceituno-Cabezas<sup>1</sup>, Hongkai Dai<sup>2</sup>, and Alberto Rodriguez<sup>1</sup>

<sup>1</sup>Department of Mechanical Engineering — Massachusetts Institute of Technology

<sup>2</sup>Toyota Research Institute

<aceituno,albertor>@mit.edu, hongkai.dai@tri.global



An illustrative example of caging, represented with blue arrows, being used to cope with uncertainty during a manipulation task.

**Abstract**—Caging is a promising tool which allows a robot to manipulate an object without directly reasoning about the contact dynamics involved. Furthermore, caging also provides useful guarantees in terms of robustness to uncertainty, and often serves as a way-point to a grasp. Unfortunately, previous work on caging is often based on computational geometry or discrete topology tools, causing restriction on gripper geometry, and difficulty on integration into larger manipulation frameworks. In this paper, we develop a convex-combinatorial model to characterize caging from an optimization perspective. More specifically, we study the configuration space of the object, where the fingers act as obstacles that enclose the configuration of the object. The convex-combinatorial nature of this approach provides guarantees on optimality, convergence and scalability, and its optimization natures makes it adaptable for further applications on robot manipulation tasks.

## I. INTRODUCTION

To cage an object is to restrict its mobility, such that the object is unable to move arbitrarily far from its initial position. Cages can also work as way-points towards a grasp [1], [2], where the object is completely immobilized, despite not being initially in contact with the object. In the context of robot manipulation, caging remains a promising tool that can enable robots to better cope with sensor induced uncertainty [1], [3] and complete manipulation tasks without complete geometric information of the object. For this reason, the ability to cage an object has been linked to potential applications in areas such as: non-prehensile manipulation [4], [5], [6], multi-robot manipulation [7], [8], and motion planning [9]. Realistically speaking, caging has retained the title of “promising tool” for decades, but without much impact within the larger manipulation community.

In the past couple of decades, significant efforts have been directed towards developing efficient algorithms to search for cages of an object. Since the concept of caging was introduced to the robotics community by Rimon and Blake [10], several algorithms able to characterize all caging configurations of a robot hand have been proposed for manipulators with two and three point fingers [11], [12]. Further work by Allen et al. [13], [14] showed how these sets could be efficiently computed by searching over the

contact space of the manipulator. Bunis et al. [15] extended the previous idea in order to efficiently find cages with a one-parameter equilateral three finger hand. Moreover, other researchers have proposed the use of scalar functions, related to dispersion of the manipulator fingers, which allow for fast cage verification on a known object [16], [2]. In recent years, more applied work has studied the use of computational topology to synthesize and verify cages on 2D and 3D objects [17], [18]. While the aforementioned approaches can generalize across objects and result computational efficiency, these are often restricted to a limited number of fingers and specific hand geometries. Moreover, it has proven difficult to integrate these algorithms as part of more complex manipulation frameworks (e.g. optimizing a trajectory through which a manipulator moves an object by caging it).

In this work, first and foremost, we develop an optimization framework for caging. This is based on a convex-combinatorial model, i.e., a model that imposes a disjunctive combination of convex constraints. Our paper presents three main contributions:

- 1) **Convex-Combinatorial model:** we propose a union of sufficient convex constraints to cage an object. The object is described as the union of convex polygons, and the gripper as an arbitrary number of fingers.
- 2) **Cage Synthesis:** using the proposed model, we formulate a cage synthesis algorithm based on numerical optimization, which can be efficiently solved with global convergence guarantees.
- 3) **Optimization Framework:** the theoretical guarantees presented allow this model to be easily adaptable for potential caging applications to areas such as planning, design and control, which are the long term objective of this work.

The remainder of this paper is organized as follows. Section II presents the main concepts and the notation used in this work. Section III provides an overview of the framework. Sections IV and V describe our convex-combinatorial model for planar caging. Section VI presents the results obtained from implementing the cage synthesis algorithm.

Finally, Section VII discusses and concludes on the contributions of this work.

## II. PRELIMINARIES

In this section we introduce the notation that we will use through the remainder of this paper. Also, we formally define the caging, as it will be treated throughout this paper.

### A. Notation

We will refer to the manipulator as  $\mathcal{M}$  and the object to cage as  $\mathcal{O}$ . The workspace of  $\mathcal{O}$  will be referred as  $\mathcal{W}$ , its configuration space or  $\mathcal{C}$ -space [19] will be referred as  $\mathcal{C}_{\mathcal{O}}$ , and its free-space in the presence of grippers [20] will be referred as  $\mathcal{C}_{\mathcal{O}_{free}}$ . Finally, the initial configuration of  $\mathcal{O}$ , in  $\mathcal{W}$ , will be referred as  $q$ . Note that the initial configurations of  $\mathcal{O}$  is the same as the origin of the space.

### B. Caging

The caging problem, based on the original formulation by Kuperberg [21], can be stated as:

*For a planar object  $\mathcal{O}$ , in a workspace  $\mathcal{W}$ , and a manipulator  $\mathcal{M}$ , described by  $N$  finger positions  $p_1, \dots, p_N \in \mathbb{R}^2$ , find a configuration of  $\mathcal{M}$  such that the object configuration  $q$  lies in a compact connected component of  $\mathcal{C}_{\mathcal{O}_{free}}$ , denoted as  $\hat{\mathcal{C}}_{\mathcal{O}_{free}}$ .*

This formulation of the problem, based on topology, is equivalent to the more traditional geometric condition that there exists no continuous path that will drive the object arbitrarily far from the manipulator, as illustrated in Fig. 1.

## III. APPROACH OVERVIEW

The caging condition described in the previous section can be transcribed as a set of mixed-integer convex conditions. For this, we make two assumptions:

- 1) The object  $\mathcal{O}$  is represented as the union of  $M$  convex polygons, covered by  $L$  facets.
- 2) The manipulator  $\mathcal{M}$  is represented as a set of  $N$  point-fingers.

To ensure that  $q$  is caged by  $\mathcal{M}$ , we will *sample* the orientation component of  $\mathcal{C}_{\mathcal{O}}$  in  $S$  slices of fixed object orientations, similar to [18], and impose that the object is caged in each slice, including continuity conditions between slices. The model uses continuous variables to represent the position of the manipulator, and binary variables to represent the discrete connectivity relationship between fingers. Then, we introduce two sets of constraints to our model:

- **At each slice:** we require that the object configuration  $q$ , i.e. Cartesian origin of  $\mathcal{C}_{\mathcal{O}}$ , lies in a compact connected component of  $\mathcal{C}_{\mathcal{O}_{free}}$  at such fixed orientations. This ensures that  $q$  is caged for all translation paths with a fixed orientation within the slice.
- **For all orientations:** we constrain that the object can only rotate between two immobilizing *limit orientations*. This ensures that the object is trapped for all rotational motion, when caging in all  $360^\circ$  is not possible. Also, we require that the  $\mathcal{C}_{\mathcal{O}_{free}}$  component

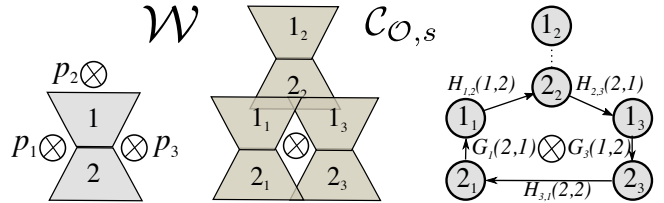


Fig. 1: The caging loop for a slice with three fingers in  $\mathcal{W}$  (left),  $\mathcal{C}_{\mathcal{O},s}$  (center) and its corresponding connection graph (right)

containing  $q$ , at a fixed orientation, transforms continuously between each pair of slices. This allows us to guarantee that all continuous  $SE(2)$  paths starting in  $q$  are enclosed by  $\mathcal{M}$ .

Throughout the paper, we will show that these conditions are sufficient to guarantee that  $q$  is caged by  $\mathcal{M}$ . Furthermore, the use of convex-combinatorial constraints allows us to provide guarantees in terms of optimality and convergence.

## IV. CAGING AT EACH SLICE

Here, we describe the set of conditions to impose caging at each orientation slice  $s$ . For notation convenience, we will refer to the translation  $\mathcal{C}$ -space of each slice as  $\mathcal{C}_{\mathcal{O},s}$  and its corresponding free-space as  $\mathcal{C}_{\mathcal{O},s_{free}}$ . For this, we require that all the fingers in  $\mathcal{C}_{\mathcal{O},s}$  create a closed curve (loop) that encloses  $q$ , such that  $q$  lies in a compact-connected component of  $\mathcal{C}_{\mathcal{O},s_{free}}$ . Since the object is decomposed in  $M$  convex polygons, the problem of finding such a loop reduces to finding a directed graph that encloses  $q$ .

1) *Existence of a loop:* In order to compose an enclosing piecewise polygonal loop, we need to determine which polygons that define the obstacle in  $\mathcal{C}_{\mathcal{O},s}$  are part of it and their direction in the graph. To this end, we represent each polygon as a node, and add an edge between two nodes if the polygons share a facet. Fig. 1 illustrates this construction. For now, and for simplicity, we assume that all fingers must be part of this loop.

Let us introduce a binary matrix  $H_{n,n+1} \in \{0,1\}^{M \times M}$ , where  $H_{n,n+1}(i,j) = 1$  if the  $i_{th}$  polygon on obstacle  $n$  intersects with the  $j_{th}$  polygon on finger  $n+1$ . Mathematically if we denote the  $i_{th}$  polygon in the  $n_{th}$  finger as  $\mathbf{P}_{i,n}$ , then we impose the constraint:

$$H_{n,n+1}(i,j) \Rightarrow \exists r_n \in \mathbb{R}^2 \text{ s.t. } r_n \in \mathbf{P}_{i,n} \cap \mathbf{P}_{j,n+1} \quad (\text{CT1})$$

where the  $\Rightarrow$  (implies) operator is transcribed into linear constraints using big-M formulation<sup>1</sup> [22]. Furthermore, to make each finger a part of the loop, we use the constraint:

$$\sum_{i,j} H_{n,n+1}(i,j) = 1, \quad \forall n \quad (\text{CT2})$$

Since the  $n_{th}$  finger intersects with the  $n_{th} + 1$  finger, for  $n = 1, \dots, m$ , there exists a directed loop of obstacles in  $\mathcal{C}_{\mathcal{O},s}$ . Then, we introduce a matrix  $G_n \in \{0,1\}^{M \times M}$  to

<sup>1</sup>For a boolean  $\mathbf{B}$ , we have  $\mathbf{B} \Rightarrow Ax \leq b$  is equivalent to  $Ax + M\mathbf{B} \leq b + M$  with  $M$  being a large positive number. This allows us to represent conditionals within the optimization model through linear constraints.

denote if an edge in the finger connection graph is in the loop. In the case that  $G_n(i, j) = 1$  the graph has an edge going from polygon  $i$  to polygon  $j$  on the  $n_{th}$  object. Algebraically, the fingers create a closed directed graph if:

$$H_{n-1,n}(i, j) \Rightarrow \exists k, l \text{ s.t. } G_n(j, k) + H_{n,n+1}(j, l) = 1 \quad (\text{CT3})$$

$$G_n(p, q) \Rightarrow \exists s, r \neq p \text{ s.t. } G_n(q, r) + H_{n,n+1}(q, s) = 1 \quad (\text{CT4})$$

(CT3) and (CT4) combined guarantee that for each node with an inbound edge, there is one outbound edge, thus we have a loop in  $\mathcal{C}_{\mathcal{O},s}$ . In the special case of a two-finger manipulator, since  $H_{n,n+1}$  and  $H_{n-1,n}$  have the same value, we need to further constrain that  $l \neq i$  in (CT3).

a) *Extension to arbitrary loops*:: The previous constraints allow us to find cages that employ all fingers. However, this model also allows for loops containing only a sub-set of the fingers. For this, we can extend the  $H$  matrix to have dimension  $M \times M(N-1)$  in order to consider all possible finger combinations. Also, constraint (CT2) would have to be relaxed and replaced by  $\sum_{i,j} \sum_n G_n(i, j) \geq 1$ , since the requirement would be to have at least one edge in the closed directed graph. This allows us to find “minimal” cages without redundant or unnecessary fingers [7].

2) *Object Enclosing*: The previous constraints ensure the existence of a compact connected component in  $\mathcal{C}_{\mathcal{O},s_{free}}$ . However, this does not guarantee that  $q$  is contained in such component. For this, we rely on the fact that enclosing  $q$  in  $\mathcal{C}_{\mathcal{O},s}$  is equivalent to enclosing the Cartesian origin of the slice. In order to incorporate this constraint to the model, will rely on Theorem 1:

**Theorem 1 (Jordan Curve Theorem [23]):** *A point  $r$  falls inside a closed curve, if and only if a linear ray that originates from  $r$  has an odd number of intersections with the closed curve.*

Constraining the number of intersections between a ray and the line segments of the enclosing curve can be formulated as a convex-combinatorial constraint. We decompose the area that covers each possible line segment of the loop into 4 square regions, parallel to the ray, and introduce a binary decision matrix  $F \in \{0, 1\}^{N \times M \times 5}$ , such that:

- 1)  $F(n, m, 1)$  through  $F(n, m, 4)$  assign  $q$  to one of four square regions enclosing the line segment starting in the

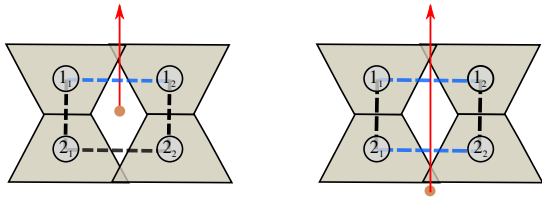


Fig. 2: A point lies within a polygon if a ray originating from that point has even number of intersections (blue) with the boundary of the polygon. Left: the point lies inside the polygon, and the ray has an odd number of intersections. Right: the point lies outside the polygon, and the ray has an even number of intersections.

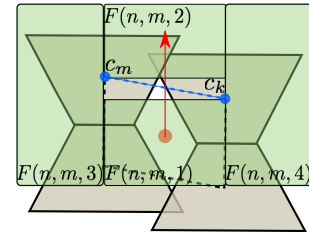


Fig. 3: Region assignment of  $q$  (red dot) depending on the value of  $F(n, m)$  and the direction of the linear ray (red arrow), for line segment going from  $c_m$  to  $c_k$  (blue). Note that, since the region is parallel to the ray, the ray always intersects the segment when  $q$  is assigned with  $F(n, m, 1)$ .

$m_{th}$  polygon of the  $n_{th}$  finger.

- 2)  $F(n, m, 5)$  is set if the  $m_{th}$  polygon of the  $n_{th}$  finger is not part of the loop.

Here, we assume that  $F(n, m, 1)$  corresponds to the region that is parallel to the ray and below the line segment. Because of this,  $F(n, m, 1) = 1$  implies that the ray intersects the segment. A visualization of this can be seen in Fig. 3. Then, we introduce the following pair of sufficient constraints:

$$\begin{cases} \sum_{n,m} F(n, m, 1) \text{ is an odd number} \\ \sum_{i=1}^5 F(n, m, i) = 1 \quad \forall n, m \end{cases} \quad (\text{CT5})$$

To transform (CT5) into a set of linear constraints, we introduce the following lemma:

**Lemma 1.** *The summation of binary variables  $\sum_{i=1}^n b_i$  is an odd number if and only if  $b_1 \text{ XOR } b_2 \dots \text{ XOR } b_n = 1$ .*

Where the XOR operator can be transcribed as linear constraints on the binary variables [24].

3) *Non-Penetration Constraints*: Additionally, we must include the condition that none of the fingers can lie in the interior of the object. For this, we partition the 2D collision free workspace  $\mathcal{W} \setminus \mathcal{O}$  into a set  $N_r$  convex regions, each of which we will represent as:

$$\mathcal{R}_i = \{x \in \mathbb{R}^2 | A_i x \leq b_i\}$$

and then constrain that each  $p_n$  finger lies in one of these regions [25], [26]. This is done by introducing the binary decision matrix  $R \in \{0, 1\}^{N_r \times N}$  such that:

$$R_{r,n} \Rightarrow A_i p_n \leq b_i \quad \text{and} \quad \sum_{r=1}^{N_r} R_{r,n} = 1, \forall n \quad (\text{CT6})$$

Where the  $\Rightarrow$  operator is represented via big-M formulation. This ensures that each finger lies in only one of the regions. Note that this constraint also ensures that  $q$  lies in the interior of  $\hat{\mathcal{C}}_{\mathcal{O},s_{free}}$  without penetrating any  $\mathcal{C}_{\mathcal{O},s}$  obstacle.

## V. FULL CAGING

In order for the object to be fully caged, the conditions presented in the previous section must be met for all continuous paths in  $\mathcal{C}_{\mathcal{O}}$ , including both rotation and translation. In this section, we present a set of sufficient conditions that guarantee that the object is fully caged for all possible motions in  $SE(2)$ .

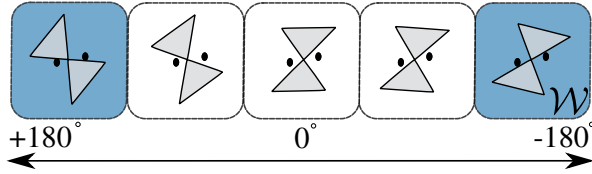


Fig. 4: Slices of the  $SE(2)$  orientation component between two limit orientations. Note that, in the *limit orientations* (blue), the object is constrained to a line of translational motion.

1) *Limit Orientations*: For most objects of interest, caging in all  $360^\circ$  cannot be achieved, since the fingers penetrate the object after some orientation. Hence, in order to ensure that the object is caged while rotating, we introduce the notion of limit orientations  $\theta_L$  as:

**Definition 3** (Limit Orientation): An object  $\mathcal{O}$  is at a limit orientation  $\theta_L$  if its free-space component at the  $\mathcal{C}$ -space slice  $\mathcal{C}_{\mathcal{O},s}$  has zero area.

In other words, a limit orientation is that at which the object's mobility is limited to translations on a line. Fig. 4 illustrates some slices between limit orientations.

To account for this, we introduce a binary variable  $\Theta \in \{0, 1\}^S$ , such that  $\Theta_s = 0$  implies that  $s_{th}$  slice has not reached a limit orientation and, thus,  $q$  must be enclosed by the loop. Then, we introduce the following constraint:

$$\begin{cases} 1 - K\Theta_s \leq \sum_{r=1}^{N_r} R_{r,n,s} \leq 1 + K\Theta_s \\ 1 - K\Theta_s \leq \sum_{i,j} H_{n,n+1}(i,j,s) \leq 1 + K\Theta_s \end{cases} \quad (\text{CT7})$$

Where  $K \in \mathbb{R}$  is a big number. Then, we constrain that  $\Theta_s = 1$  when the component of  $\mathcal{C}_{\mathcal{O}_{free}}$  in the slice gets reduced to zero area. Moreover, assuming slices are ordered by increasing orientation, we add the condition that  $\Theta_s = 1$  implies  $\Theta_{s+1} = 1$  for positive orientations and  $\Theta_{s-1} = 1$  for negative ones. Reaching this condition is dependent on the number of fingers and the  $L$  facets of the object. Seen from  $\mathcal{W}$ , this zero-area condition is reached when:

- 1) Two fingers: the fingers make contact with 2 opposite facet of the object, as in Fig. 4.
- 2) Three or more fingers: either three of the fingers are in contact with non-co-directional facets or two of the fingers are in contact with opposite facets.

Here, opposite refers to facets with parallel normals and opposite direction, while co-directional refers to facets with the same normal vector. It is important to note that, since the gripper surrounds  $\mathcal{O}$ , *concave vertices* in the object can be considered opposite to any facet.

Finally, in order to determine when a limit orientation has been reached, we introduce a binary matrix  $T \in \{0, 1\}^{N \times L \times S}$ , such that  $T_{n,f,s} = 1$  implies that the  $n_{th}$  finger is in contact with facet  $f$  at the  $s_{th}$  slice. Depending on the object and the number of fingers, the  $T$  matrix will be constrained to determine when a limit orientation has been reached. Denoting  $\mathcal{L}_{\mathcal{O}}$  as the set of facet assignments

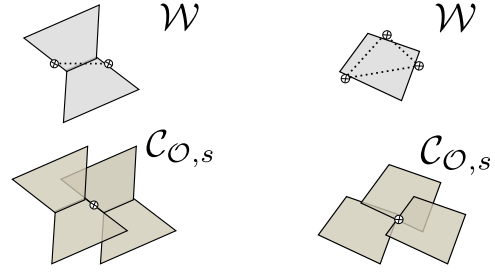


Fig. 5: Two examples of limit orientations being reached for two fingers (left: two opposite facet) and three fingers (right: three non-co-directional facets).

resulting in a limit orientation, we constrain:

$$T_s \in \mathcal{L}_{\mathcal{O}} \Rightarrow \Theta_s = 1 \quad (\text{CT8})$$

Examples of the contact conditions required to reach a limit orientation can be seen in Fig. 5. The idea of caging between two limit configurations can be seen as equivalent to finding a critical point of the inter-finger distance function in the contact space of the object [13], [15].

2) *Continuous Boundary Variation*: The constraints described above are necessary and sufficient to ensure that each slice is caged for translational motions. However, escaping paths might still exist in  $SE(2)$ , where orientation changes along with the motion [2]. To avoid this, we propose a sufficient condition, which ensures that all possible  $SE(2)$  path of  $\mathcal{O}$  lie in a compact connected component of  $\mathcal{C}_{\mathcal{O}_{free}}$ . As a start, we define the notion of a component boundary:

**Definition 4** (Component Boundary): Given a closed geometric component  $C$ , we define its boundary  $\partial(C)$  as the closed curve in the interior of the component with the largest enclosing area contained within the curve.

Let us define the map  $f(C, \theta) : C \times \mathbb{R} \rightarrow \partial(C)$ , which parametrizes the boundary of a component  $C$  depending on a variable  $\theta$ . Also, we introduce the function  $\delta_H(\partial(C_1), \partial(C_2)) : \partial(C) \times \partial(C) \rightarrow \mathbb{R}$  which returns the Hausdorff distance between two boundaries  $C_1$  and  $C_2$ . Finally, we say that the boundary of  $C$  *varies continuously* with respect to a variable  $y$  if  $\lim_{\Delta y \rightarrow 0} \delta_H(f(C, y), f(C, y + \Delta y)) = 0$ . Then, as the basis for ensuring caging for all  $SE(2)$  motions, let us propose Theorem 2:

**Theorem 2** (Continuous Boundary Variation). *The configuration of an object  $\mathcal{O}$  which lies in a compact connected component of a sliced  $\mathcal{C}_{\mathcal{O}_{free}}$ , with a geometric boundary  $\partial(\hat{\mathcal{C}}_{\mathcal{O}_{free}})$  that changes continuously through variations in the orientation of  $\mathcal{O}$ , will always lie in a compact connected component of the continuous  $\mathcal{C}_{\mathcal{O}_{free}}$ .*

*Proof.* For any component with a geometric boundary that changes continuously via parametric changes, such boundary either contracts or expands. Because of this, in the  $\mathcal{C}$ -space for all orientations in the range between a pair  $\phi_1$  and  $\phi_2$ , if  $\partial(\hat{\mathcal{C}}_{\mathcal{O}_{free}})$  *varies continuously* with respect to the orientation of  $\mathcal{O}$ , then the area in the interior of  $\partial(\hat{\mathcal{C}}_{\mathcal{O}_{free}})$  will also change continuously. Since orientations are periodical, either

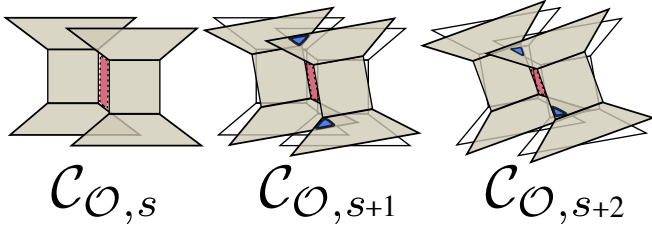


Fig. 6: If there is a continuous intersection between the connecting polygons (blue) in adjacent slices, there is a continuous variation of the compact-connect component of  $\mathcal{C}_{O_{free}}$  (red).

the area in the interior of  $\partial(\hat{\mathcal{C}}_{O_{free}})$  varies continuously between two limit orientations or it contracts and expands periodically. Hence, regardless of the  $SE(2)$  continuous path, there is always a volume in  $\mathcal{C}_O$  that will prevent  $\mathcal{O}$  from escaping. Therefore,  $q$  lies in a compact connected component of  $\mathcal{C}_{O_{free}}$ .

A similar notion, in the case of three discs, is used in [27]. By applying Theorem 2, we can guarantee that the object remains caged in all  $\mathcal{C}_O$ . A simple convex constraint to ensure continuous boundary variation, is to require the same discrete connections between polygons at each slice remain connected in adjacent slices, as shown in Fig. 6.

A sufficient condition to guarantee continuous boundary variation is that there is a point fixed in  $n_{th}$  finger, that remains always in the intersection area between the  $i_{th}$  polygon on finger  $n$  and  $j_{th}$  polygon on finger  $n+1$ , during the rotation between two adjacent slices  $s$  and  $s+1$ , as depicted in Fig. 7. We denote this point as  $x$ , and introduce its position fixed to  $\mathbf{P}_{j,n+1}$  as  $^{j,n+1}x$ . To constrain point  $x$  to be in the intersection region, we first impose the constraint:

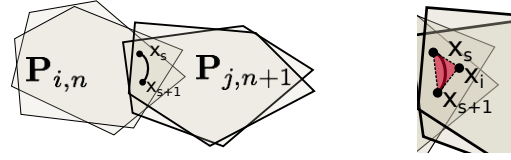
$$^{j,n+1}x \in \mathbf{P}_{j,n+1} \quad (\text{CT9})$$

such that  $x$  is always in  $\mathbf{P}_{j,n+1}$ . On the other hand, to constrain that point  $x$  remains in  $\mathbf{P}_{i,n}$  during rotation  $\theta \in [\theta_s, \theta_{s+1}]$ , we consider the trajectory of  $x$  expressed in  $\mathbf{P}_{i,n}$ 's coordinate as a function of  $\theta$ :

$$^{i,n}x(\theta) = ^{j,n+1}x + R(\theta)^T(c_{j,n+1} - c_{i,n})$$

where  $R(\theta) \in \mathbb{R}^{2 \times 2}$  is the rotation matrix for angle  $\theta$ , and  $c_{j,n+1}, c_{i,n}$  are the decision variables representing the position of  $\mathbf{P}_{i,n}$  and  $\mathbf{P}_{j,n+1}$  respectively. Hence,  $^{i,n}x(\theta)$  is an arc on a circle, drawn in Fig.7, and we require that this arc is in  $\mathbf{P}_{i,n}$ . To enforce arc enclosing within the polygon as a convex constraint, we formulate the stronger condition that the two ends ( $x_s = ^{i,n}x(\theta_s), x_{s+1} = ^{i,n}x(\theta_{s+1})$ ) of the arc, together with the intersection point  $x_i$  between the tangent lines at two ends, are all in the polygon. Since the arc is always within the triangle formed by these three points, it is thus guaranteed that the arc lies in  $\mathbf{P}_{i,n}$  (Fig.7b). The positions of  $x_s$  and  $x_{s+1}$  can be written as linear functions of the decision variables. The position of  $x_i$  can be computed as:

$$x_i = x_s + \left( \mathbf{I}_{2 \times 2} + R(-90^\circ) \tan \frac{\theta_{s+1} - \theta_s}{2} \right) (c_{j,n+1} - c_{i,n}) \quad (\text{CT10})$$



(a) Arc trajectory of a point between two adjacent slices (b) Enveloping polygon of the arc

Fig. 7: In order to avoid that the loop breaks between slices, we require that the trajectory of the intersection point  $x$  in between slices to lie in  $\mathbf{P}_{j,n+1}$ .

again as a linear function of our decision variables. We activate the constraints above when the two polygons are intersecting, as:

$$H_{n,n+1,s}(i,j) \Rightarrow x_s, x_{s+1}, x_i \in \mathbf{P}_{i,n} \quad (\text{CT11})$$

Through this constraint, we ensure that the intersection polygons of  $\mathcal{C}_{O,s}$  remain connected for all orientations between  $\mathcal{C}_{O,s}$  and  $\mathcal{C}_{O,s+1}$ . Hence, the free-space component boundary only expands or contracts continuously when rotating between slices. Note that, since the boundary of the free-space component changes continuously, it is sufficient to enforce the origin enclosing constraints (CT5) in one of the slices, instead of all slices. Thus, we can significantly reduce the number of the binary variables, achieving better scalability of the approach.

## VI. IMPLEMENTATION AND RESULTS

In this section we implement an optimization-based cage-finding algorithm, derived from the proposed model. Then, we test the tractability of this formulation by synthesizing cages for different planar geometries.

### A. Formulating Caging as Optimization

The cage finding problem, originally presented in [21], can be solved as an optimization problem using the proposed model. In this case, an optimization solver must be able to find a cage for an arbitrary object. Given an object segmented in  $M$  polygons, a manipulator with  $N$  fingers and sampling  $\mathcal{C}_O$  in  $S$  orientation layers, we formulate the cage-finding algorithm as the feasibility problem **MIP1**.

$$\mathbf{MIP1} : \underset{\Theta, H, G, R, T}{\text{find}} \quad p_1, \dots, p_N$$

subject to:

- 1) For all  $S$  slices:
  - Existence of a loop (CT1)—(CT4).
  - Non-penetration (CT6).
  - Limit orientation constraints (CT7)—(CT8).
- 2) For slice  $s = 0^\circ$ :
  - Configuration enclosing (CT5).
- 3) Continuous Boundary Variation (CT9)—(CT11).

Through this formulation, we apply our model to find cages on planar objects, with an arbitrary number of fingers.

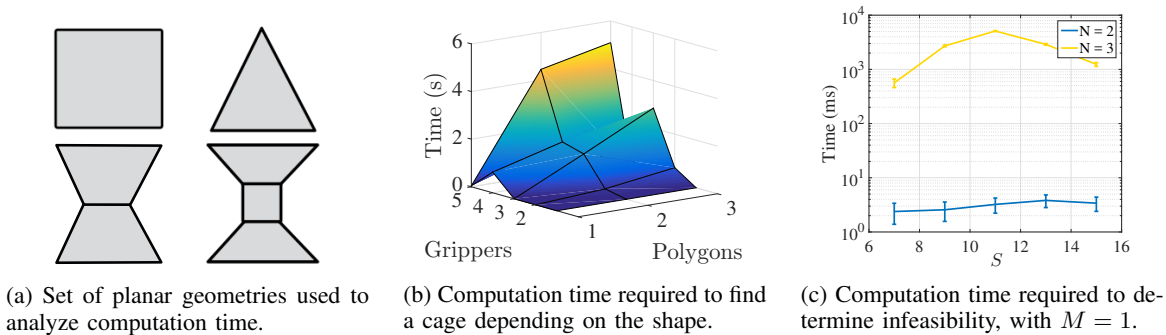


Fig. 8: Computation time analysis for cage synthesis with our convex-combinatorial model

### B. Results and Complexity Analysis

In order to test the proposed cage-finding formulation, we transcribe the optimization problem as a Mixed-Integer Program (MIP) and solve it using off-the-self optimization software. All the tests are performed in MATLAB 2015a, on a Dual-Core Laptop running Mac OS X High Sierra. We use Gurobi 8.0.0 [28] as our MIP solver. For all tests, we set the parameter  $S$  to 9 slices, evenly distributed in a range between  $-90^\circ$  and  $90^\circ$ . Fig. 9 shows an example of a cage found with this approach, on a non-intuitive object where increasing finger dispersion does not guarantee a cage [2]. To illustrate some of the capabilities of this approach, Fig. 10 shows the resulting cages under different constraints, including: unconstrained caging, caging with a fixed finger and caging with a set distance between fingers.

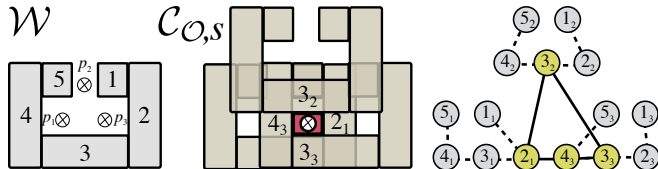


Fig. 9: Example cage found with **MIP1** in the workspace (left), configuration space slice (center) and its connection graph (right).

We assess the scalability of the optimization problem by comparing the computation time required to solve **MIP1** in a set of different objects, shown in Fig. 8a. For each object, we test computation time using a set from two to five point fingers. After running the feasibility problem for each geometry, the reported results are presented in Fig. 8b. Note that, in the worst case, a solution to the problem is found in under 6 seconds. Additionally, when caging an object is not possible (e.g. a square with two fingers), the solver is able to report infeasibility in a range from 2 *ms* to 5 *s*, as shown in Fig. 8c, depending on the size of the MIP.

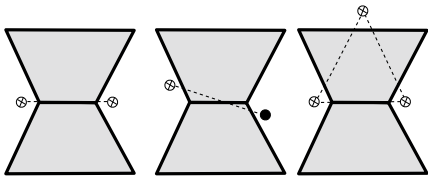


Fig. 10: Examples of resulting cages under different constraints: 2-finger caging (left), caging with a finger and a fixed black point (center), caging with fingers in a triangle (right).

## VII. CONCLUSIONS

In this paper, we have presented a novel convex-combinatorial model for planar caging, able to reason over arbitrary planar shapes with an arbitrary number of fingers. The formulation is based on a set of sufficient conditions which can be transcribed as convex and combinatorial constraints within an optimization problem. To the best of our knowledge, this is the first optimization-based approach to formulate the caging condition. A key contribution of the work is the potential of the formulation to be compatible with other task constraints. For example: to further constrain the kinematics of the manipulator [29] (e.g. coupled grippers), environment use [30] (e.g. caging with a wall), and reaching motions [2] (e.g. reach  $\rightarrow$  cage  $\rightarrow$  grasp). Furthermore, we have shown how to implement the cage-synthesis algorithm derived from our model, easily solvable as an MIP. Our implementation results showcase the scalability properties of this approach, despite the combinatorial nature of the formulation.

### A. Future Work

Future efforts will aim to reduce the complexity of the model, currently exponential in the worst case. This can potentially be done through the introduction of stronger conditions that reduce the combinatorial elements in the formulation. Furthermore, while the conditions in this paper are sufficient to guarantee caging, in particular those derived from Theorem 2, we suspect that these could also become necessary and sufficient through a dense enough sampling. This potential "resolution completeness" property of the model should be explored in the future. Finally, extending this model to handle caging of 3D objects in  $SE(3)$  is a natural future direction to pursue.

### B. Source Code

The entire source code used as part of this work is publicly available on GitHub: <https://github.com/baceituno>

## ACKNOWLEDGMENTS

We would like to thank Anastasiia Varava, José Camacho, Sean Curtis and members of the MCube Lab for insightful discussions and advice during the development of this project.

## REFERENCES

- [1] W. Wan, R. Fukui, M. Shimosaka, T. Sato, and Y. Kuniyoshi, "Grasping by caging: A promising tool to deal with uncertainty," in *ICRA*. IEEE, 2012.
- [2] A. Rodriguez, M. T. Mason, and S. Ferry, "From caging to grasping," *IJRR*, 2012.
- [3] D. Hirano, H. Kato, and N. Tanishima, "Caging-based grasp with flexible manipulation for robust capture of a free-floating target," in *ICRA*. IEEE, 2017.
- [4] A. Sudsang and J. Ponce, "A new approach to motion planning for disc-shaped robots manipulating a polygonal object in the plane," in *ICRA*. IEEE, 2000.
- [5] J. Mahler, F. T. Pokorny, Z. McCarthy, A. F. van der Stappen, and K. Goldberg, "Energy-bounded caging: Formal definition and 2-d energy lower bound algorithm based on weighted alpha shapes," *Robotics and Automation Letters*, 2016.
- [6] J. Seo, M. Yim, and V. Kumar, "A theory on grasping objects using effectors with curved contact surfaces and its application to whole-arm grasping," *IJRR*, 2016.
- [7] G. A. Pereira, M. F. Campos, and V. Kumar, "Decentralized algorithms for multi-robot manipulation via caging," *IJRR*, 2004.
- [8] A. Varava, K. Hang, D. Kragic, and F. T. Pokorny, "Herding by caging: a topological approach towards guiding moving agents via mobile robots," in *RSS*, 2017.
- [9] R. Diankov, S. S. Srinivasa, D. Ferguson, and J. Kuffner, "Manipulation planning with caging grasps," in *Humanoids*. IEEE, 2008.
- [10] E. Rimon and A. Blake, "Caging 2d bodies by 1-parameter two-fingered gripping systems," in *ICRA*. IEEE, 1996.
- [11] P. Pipattanasomporn and A. Sudsang, "Two-finger caging of concave polygon," in *ICRA*. IEEE, 2006.
- [12] M. Vahedi and A. F. van der Stappen, "Caging polygons with two and three fingers," *IJRR*, 2008.
- [13] T. F. Allen, J. W. Burdick, and E. Rimon, "Two-finger caging of polygonal objects using contact space search," *Transactions on Robotics*, 2015.
- [14] T. F. Allen, E. Rimon, and J. W. Burdick, "Robust three-finger three-parameter caging of convex polygons," in *ICRA*. IEEE, 2015.
- [15] H. A. Bunis, E. D. Rimon, T. F. Allen, and J. W. Burdick, "Equilateral three-finger caging of polygonal objects using contact space search," *Transactions on Automation Science and Engineering*, 2018.
- [16] P. Pipattanasomporn, P. Vongmasa, and A. Sudsang, "Caging rigid polytopes via finger dispersion control," in *ICRA*. IEEE, 2008.
- [17] A. Varava, D. Kragic, and F. T. Pokorny, "Caging grasps of rigid and partially deformable 3-d objects with double fork and neck features," *Transactions on Robotics*, 2016.
- [18] A. Varava, J. F. Carvalho, F. T. Pokorny, and D. Kragic, "Caging and path non-existence: a deterministic sampling-based verification algorithm," in *ISRR*, 2017.
- [19] T. Lozano-Perez, "Spatial planning: A configuration space approach," *IEEE Transactions on Computers*, 1983.
- [20] A. Rodriguez and M. T. Mason, "Path-connectivity of the free space," *Transactions on Robotics*, 2012.
- [21] W. Kuperberg, "Problems on polytopes and convex sets," in *DIMACS Workshop on polytopes*, 1990, pp. 584–589.
- [22] A. Richards and J. How, "Mixed-integer programming for control," in *ACC*. IEEE, 2005.
- [23] H. Tverberg, "A proof of the Jordan curve theorem," *Bulletin of the London Mathematical Society*, 1980.
- [24] D. (<https://cs.stackexchange.com/users/755/dw>), "Express boolean logic operations in zero-one integer linear programming (ilp)," *Computer Science Stack Exchange*.
- [25] R. Deits and R. Tedrake, "Computing large convex regions of obstacle-free space through semidefinite programming," in *WAFR*. Springer, 2015.
- [26] —, "Efficient mixed-integer planning for uavs in cluttered environments," in *ICRA*. IEEE, 2015.
- [27] J. Erickson, S. Thite, F. Rothganger, and J. Ponce, "Capturing a convex object with three discs," *Transactions on Robotics*, 2007.
- [28] I. Gurobi Optimization, "Gurobi optimizer reference manual," 2018. [Online]. Available: <http://www.gurobi.com>
- [29] H. Dai, G. Izatt, and R. Tedrake, "Global inverse kinematics via mixed-integer convex optimization," in *ISRR*, 2017.
- [30] C. Eppner, R. Deimel, J. Ivarez Ruiz, M. Maertens, and O. Brock, "Exploitation of environmental constraints in human and robotic grasping," *IJRR*, 2015.